

**A Shorter Duration of Indian Summer Monsoon in Constrained Projection**

Yifeng Cheng<sup>1</sup>, Lu Wang<sup>1,2\*</sup>, Xiaolong Chen<sup>3</sup>, Tianjun Zhou<sup>3,4</sup>, Andrew Turner<sup>5,6</sup>

<sup>1</sup>Key Laboratory of Meteorological Disaster, Ministry of Education (KLME) / Collaborative Innovation Center on Forecast and Evaluation of Meteorological Disasters (CIC-FEMD), Nanjing University of Information Science and Technology, Nanjing, China.

<sup>2</sup>Laboratory for Regional Oceanography and Numerical Modeling, Qingdao Marine Science and Technology Center, Qingdao, China.

<sup>3</sup>State Key Laboratory of Numerical Modeling for Atmospheric Sciences and Geophysical Fluid Dynamics, Institute of Atmospheric Physics, Chinese Academy of Sciences, Beijing, China.

<sup>4</sup>College of Earth and Planetary Sciences, The University of Chinese Academy of Sciences, Beijing, China.

<sup>5</sup>National Centre for Atmospheric Science, University of Reading, Reading, UK.

<sup>6</sup>Department of Meteorology, University of Reading, Reading, UK.

**Contents of this file**

Text S1

Table S1

Figures S1 to S4

**Introduction**

The supporting information describes the hierarchical statistical framework for emergent constraints (see Text S1), and information about the 24 CMIP6 models used in this study (see Table S1) are also listed.

## Text S1. Hierarchical statistical framework for emergent constraint

The hierarchical emergent constraint framework proposed by Bowman et al. (2018) is used to constrain the projection uncertainty of monsoon onset and withdrawal. In this framework, we should establish a connection between future climate change  $Y$  and current climate  $X$  to constrain  $Y$ . The connection between  $Y$  and  $X$  can be obtained by applying linear regression to climate models, that is:

$$Y = \bar{Y} + \rho(X - \bar{X}), \quad (1)$$

where  $\rho$  is the regression coefficient,  $\bar{X}$  and  $\bar{Y}$  are the multi-model mean of  $X$  and  $Y$ , respectively.

Since  $Y$  is constrained by the observed  $X$  in the current climate ( $X_O$ ), the uncertainty in observations should be considered. Under the Gaussian assumption that relates the observations to current climate, the signal-noise ratio (SNR) in the observation is the ratio between the variance among modes ( $\sigma_X^2$ ) and observational datasets ( $\sigma_O^2$ ):

$$\text{SNR} = \sigma_X^2 / \sigma_O^2, \quad (2)$$

The regression coefficient  $\rho$  is corrected by multiplying  $\frac{1}{1+\text{SNR}^{-1}}$ . If the SNR is large enough ( $\text{SNR} \gg 1$ ), the effect of correction can be neglected. Hence, combining Eqs. (1) and (2), the constrained projection and variance of future climate change  $Y_C$  can be written as:

$$\bar{Y}_C = \bar{Y} + \frac{\rho}{1+\text{SNR}^{-1}} (\bar{X}_O - \bar{X}), \quad (3)$$

$$\sigma_{Y_C}^2 = (1 - \frac{r^2}{1+\text{SNR}^{-1}}) \sigma_Y^2, \quad (4)$$

where  $r$  is the correlation coefficient between  $X$  and  $Y$ . Based on Eq. (4), the relative variance reduction ( $1 - \frac{\sigma_{Y_C}^2}{\sigma_Y^2}$ ) derived from the hierarchical statistical framework is  $\frac{r^2}{1+\text{SNR}^{-1}}$ .

44 **Table S1.** Basic information of 24 CMIP6 models used in this study.

Model Name	Institute/Country
ACCESS-CM2	CSIRO/Australia
ACCESS-ESM1-5	CSIRO/Australia
CanESM5	CCCma/Canada
CESM2-WACCM	NCAR/USA
CMCC-CM2-SR5	CMCC/Italy
CMCC-ESM2	CMCC/Italy
EC-Earth3	EC-Earth-Consortium/Europe
EC-Earth3-CC	EC-Earth-Consortium/Europe
EC-Earth3-Veg	EC-Earth-Consortium/Europe
EC-Earth3-Veg-LR	EC-Earth-Consortium/Europe
FGOALS-g3	CAS/China
GFDL-CM4	NOAA-GFDL/USA
IITM-ESM	CCCR-IITM/India
INM-CM4-8	INM/Russia
INM-CM5-0	INM/Russia
IPSL-CM6A-LR	IPSL/France
MIROC6	MIROC/Japan
MPI-ESM1-2-HR	MPI-M/Germany
MPI-ESM1-2-LR	MPI-M/Germany
MRI-ESM2-0	MRI/Japan
NESM3	NUIST/China
NorESM2-LM	NCC/Norway
NorESM2-MM	NCC/Norway
TaiESM1	AS-RCEC/China

45

46

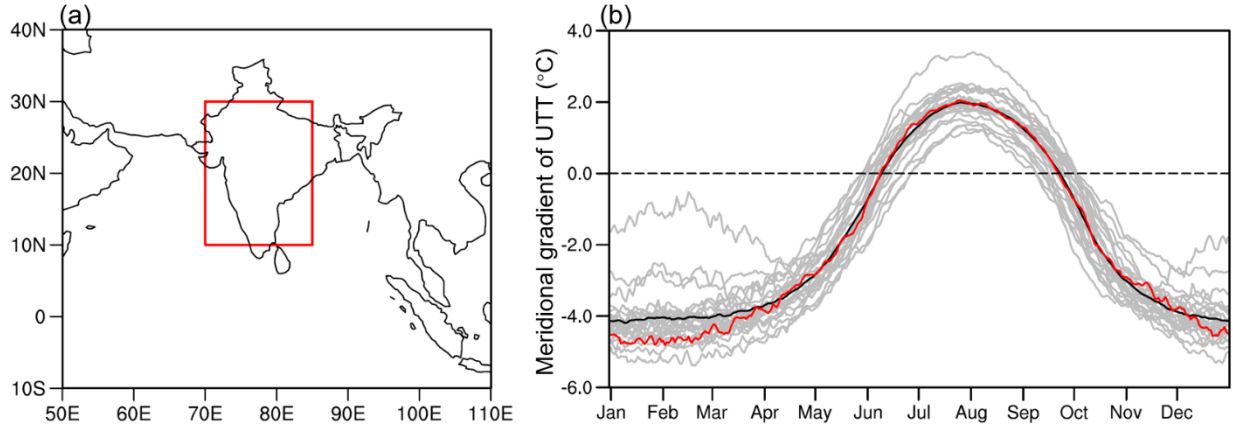


**Figure S1.** (a) Map showing the region (red box; 10°-30°N, 70°-85°E) used to calculate the meridional gradient of UTT (°C). (b) Seasonal evolution of daily climatology of meridional UTT gradient for the observations (red curve), multi-model mean of CMIP6 historical simulations (black curve) and individual model results (gray curves).

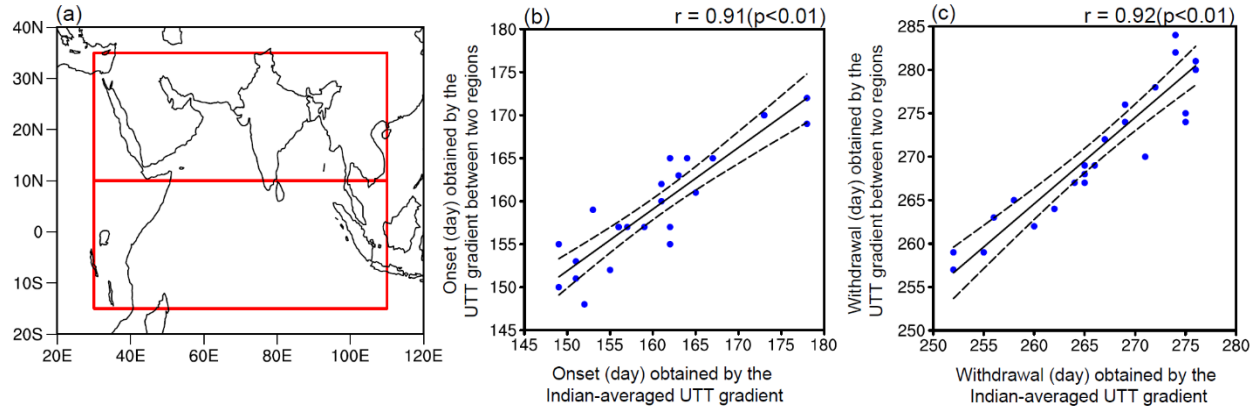


**Figure S2.** (a) Map showing the northern region (10°-35°N; 30°-110°E) and the southern region (15°S-10°N; 30°-110°E). The difference of UTT (°C) between the northern region and the southern region is calculated as the meridional gradient of UTT. The simulated (b) onset (day) and (c) withdrawal (day) of Indian summer monsoon among models. The onset and withdrawal dates are obtained by the Indian-averaged UTT gradient and the UTT difference between the northern and southern regions. The best-fit line (solid black) is obtained by the least-squares method, and dashed curves represent the 95% confidence range of the linear fit. The inter-model correlation coefficient ( $r$ ) and p-value are shown on the top-right corner.

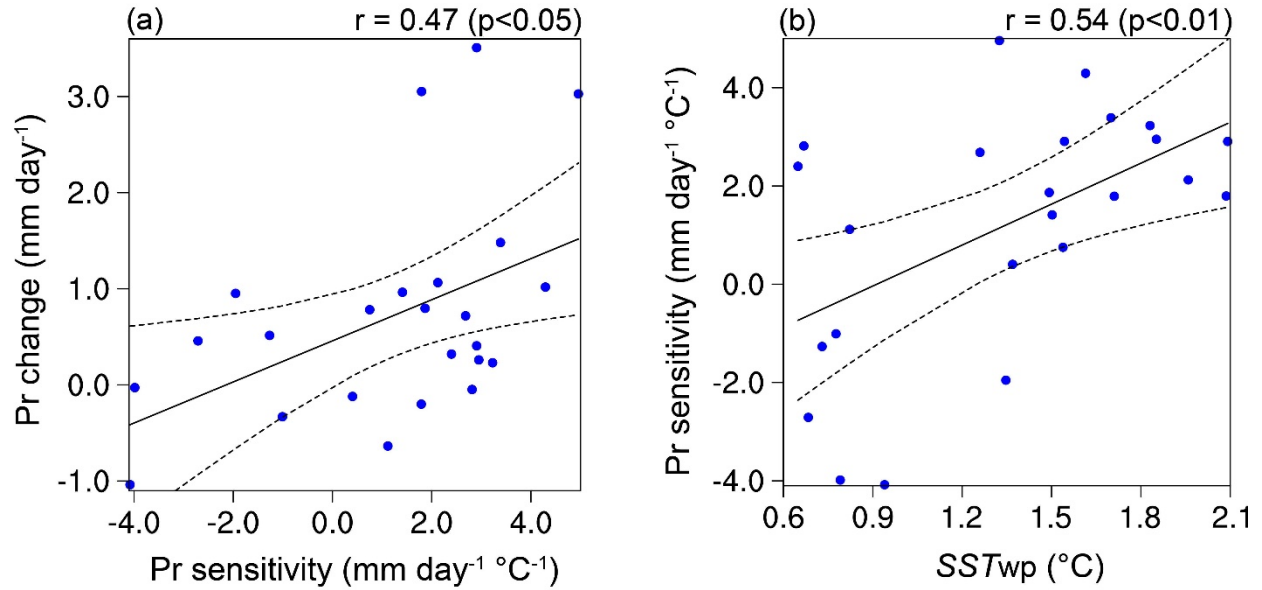


**Figure S3.** Inter-model relationships of the current precipitation sensitivity (mm day<sup>-1</sup> °C<sup>-1</sup>) over the equatorial western-central Pacific (5°S-5°N, 140°-170°E) versus (a) local precipitation change (mm day<sup>-1</sup>) and (b) SST<sub>WP</sub> (°C) during spring. The solid best-fit line is obtained using the least-squares method, and dashed curves represent the 95% confidence range of the linear fit. The inter-model correlation coefficient ( $r$ ) and p-value are shown in the top right corner.

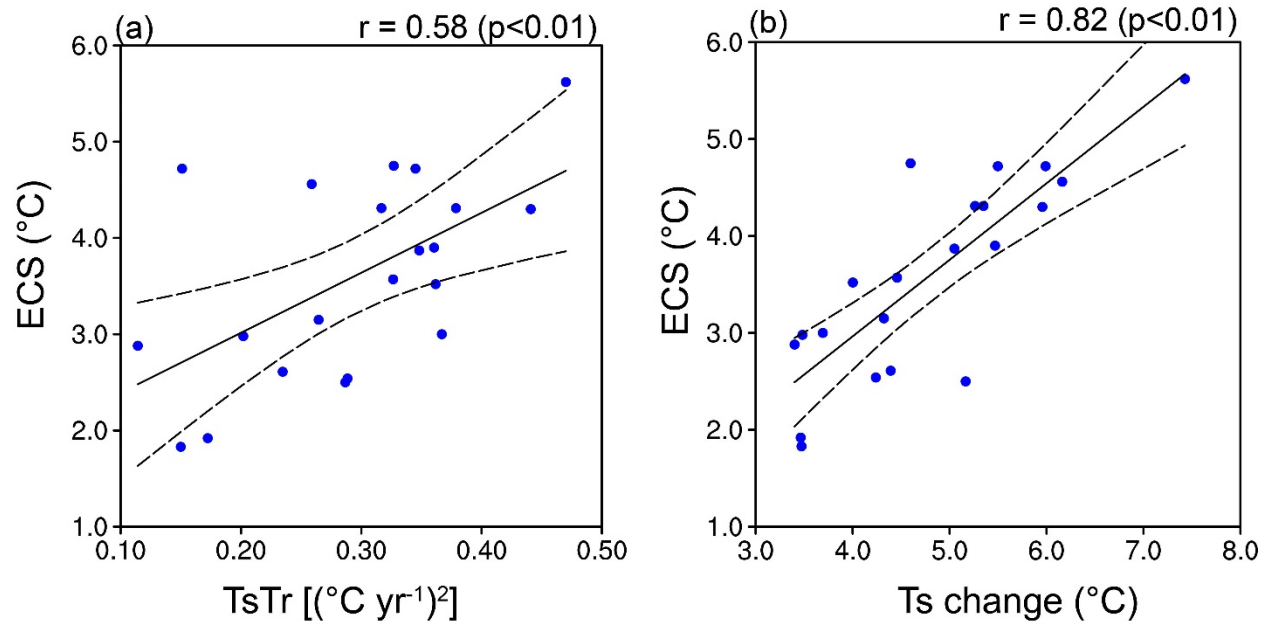


**Figure S4.** Inter-model relationships of the equilibrium climate sensitivity (ECS; °C) versus (a) TsTr [(°C yr<sup>-1</sup>)<sup>2</sup>] and (b) Ts change (°C) averaged over the NMHL (30°-70°N, 0-360°E) during autumn. The solid best-fit line is obtained using the least-squares method, and dashed curves represent the 95% confidence range of the linear fit. The inter-model correlation coefficient ( $r$ ) and p-value are shown in the top right corner.

## References

Bowman, K. W., Cressie, N., Qu, X., & Hall, A. (2018). A hierarchical statistical framework for emergent constraints: application to snow-albedo feedback. *Geophysical Research Letters*, 45(3), 13050-13059. <https://doi.org/10.1029/2018GL080082>